

# RF DESIGN OF A COMPACT C-BAND RF PULSE COMPRESSOR FOR A VHEE LINAC FOR FLASH RADIOTHERAPY

G. Torrisi\*, G. S. Mauro, G. Sorbello<sup>2</sup>, INFN-LNS, Catania, Italy

L. Faillace, B. Spataro, INFN Laboratori Nazionali di Frascati, Italy

L. Giuliano<sup>5</sup>, M. Migliorati<sup>5</sup>, A. Mostacci<sup>5</sup>, L. Palumbo<sup>5</sup>, SBAI, Sapienza University of Rome, Italy

<sup>2</sup>also at University of Catania, Catania, Italy

<sup>5</sup>also at INFN-Sezione di Roma, Italy

## Abstract

In this paper, the design of a compact C-band RF Pulse Compressor for a Very High Electron Energy (VHEE) FLASH machine is presented. A spherical cavity RF pulse compressor – selected because of its compactness and relative ease of fabrication – is adopted to compress the 50 MW, 3  $\mu$ s RF pulse, down to 0.3  $\mu$ s obtaining a peak power gain greater than 7. The main characteristics (operating resonant mode, unloaded quality factor, coupling factor, peak power gain, peak surface fields) as well as the scattering parameters of the full RF design (spherical storage cavity and mode converter/polarizer) are computed and analyzed. Moreover, the pulse-compression effect on the acceleration performances is analyzed through the evaluation of the main figures of merit (charge per pulse, energy gain, accelerating gradient and efficiency).

## INTRODUCTION AND MOTIVATION

This paper presents the RF design and simulations of a C-band (5.712 GHz) spherical pulse compressor for a Very High Electron Energy (VHEE) FLASH machine. VHEE [1] irradiations could represent a valid technique to apply the FLASH effect [2] in clinical use to treat deep tumors. The design of the C-band VHEE FLASH LINAC aiming at reach high accelerating gradient ( $> 40$  MV/m), current  $> 200$  mA and beam energy  $> 50$  MeV, necessary to deliver a Ultra High Dose Rate with a beam pulse duration of 3  $\mu$ s has been presented in [3, 4]. The output beam energy can be increased by enhancing the RF peak power at the expense of RF pulse width by using a pulse compressor. This system called “SLAC Energy Doubler (SLED)” was firstly proposed and applied in [5]; then it has been widely used elsewhere also according different schemes such as the Binary Pulse Compression (BPC) [6], SLED-II [7], Barrel Open Cavity (BOC) pulse compressor [8] and single spherical cavity pulse compressor – adopted at SLAC for an X-band transverse RF deflector system [9] – which is also the one selected in this work. The spherical cavity pulse compressor belongs to the SLED-like pulse compressor family, but it is composed of a “special” 3 dB coupler (also acting as a circular polarizer) and make use of a single spherical energy storage cavity compared with the traditional SLED where two cylindrical cavities are adopted. This spherical pulse compressor is also

more compact while keeping a high energy gain and  $Q$  factor with a simpler cooling system.

As reported in Fig. 1 (a), in order to reach the design range of energy ( $> 50$  MeV), the LINAC is powered by a 50 MW klystron providing a RF pulse of 3  $\mu$ s at a repetition frequency rate of 100 Hz[10]. Part of the power,  $\sim 3$  MW, is used for the injector while the remaining one feeds the accelerating structure which would accelerate a total charge of 600 nC at a maximum energy of 60 MeV without (w/o) pulse compressor as listed in Tab. 1 left column. On the other hand, in Fig. 1 (b), the layout in presence of the RF pulse compressor is shown. Indeed, in order to reach a higher energy, the system is equipped with a pulse compressor which compresses the RF pulse to less than 0.5  $\mu$ s such to multiply the available power by a factor greater than 3. The corresponding pulse charge of 200 nC is accelerated at a maximum energy of 100 MeV (see the right column of Tab. 1).

Table 1: Parameters without (w/o) and with RF Pulse Compressor

Parameter	w/o	with Pulse Compressor
Beam Energy	60 MeV	100 MeV
Pulse Width	3 $\mu$ s	0.3 $\mu$ s
Pulse charges	600 nC	200 nC
RF Power	50 MW	150 MW
Acc. Gradients	$\sim 40$ MV/m	$\sim 60$ MV/m
Beam Current	$\geq 200$ mA	$\geq 50$ mA
Structure length	$\sim 0.9$ m	$\sim 0.9$ m

## RF DESIGN OF THE SPHERICAL PULSE COMPRESSOR

The two subsystems of the spherical pulse compressor – that are a special 3 dB coupler (or circular polarizer) and a spherical storage cavity [11] – have been firstly designed separately by the simulation software CST MW Studio ®2022 and then assembled together to simulate the complete device. Hereinafter the details of the design.

### 3 dB Coupler-Polarizer

The 3 dB coupler acts as a circular polarizer since converts the rectangular TE<sub>10</sub> input mode (Port 1) from klystron to the two equal amplitude and 90° phase difference TE<sub>11</sub> (orthogonal) degenerated modes in the cylindrical waveguide

\* giuseppe.torrisi@lns.infn.it

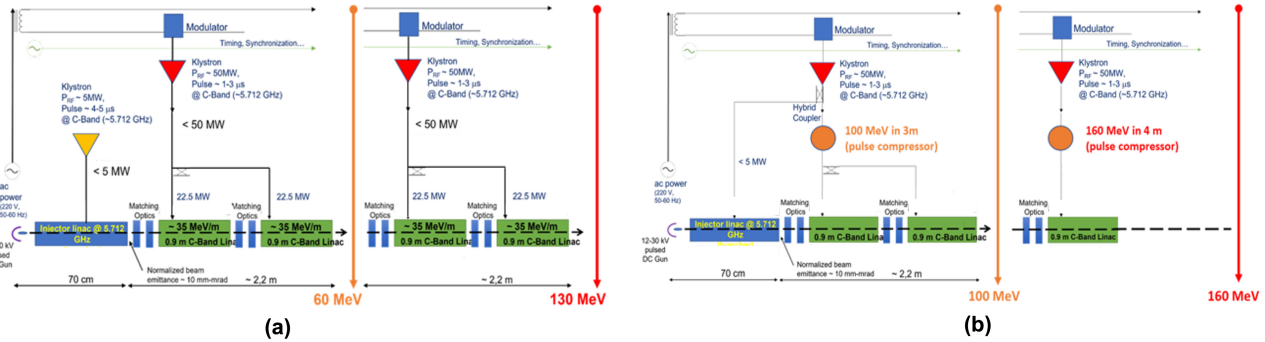


Figure 1: Layout comparison of the C-band accelerator for VHEE FLASH radiotherapy without (a) and with (b) pulse compressor[3, 4].

port (Port 3) of the spherical storage cavity. The simulated electrical field distribution and the S-parameters obtained by using CST software are shown in Fig. 2 and 3, respectively.

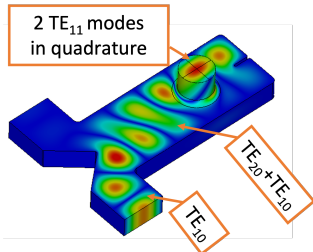


Figure 2: Simulated electrical field distribution showing the rectangular  $TE_{10}$  input mode and the  $TE_{11}$  mode on the circular waveguide

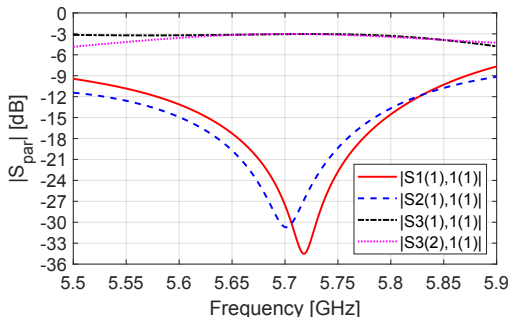


Figure 3: S-parameters of the 3dB hybrid-polarizer.

The two in-quadrature/orthogonal  $TE_{11}$  modes of the circular waveguide are excited by the two  $TE_{10}$  and  $TE_{20}$  modes propagating in the overmoded waveguide section which has an optimized width. The proper amplitude and phase of the two  $TE_{11}$  modes have been optimized acting on the position of the circular waveguide. The simulated S parameters show that the reflection  $|S1(1),1(1)|$  and isolation  $|S2(1),1(1)|$  are both below  $-30$  dB and the input wave is equally splitted at the circular output port 3, generating two  $TE_{11}$  modes with phase difference  $90^\circ$  between each other at the operating frequency of  $5.721$  GHz. The maximum electric field is around  $12$  MV/m at the beginning of the circular waveguide

section when the input power is  $50$  MW (Kilpatrick Limit is  $62$  MV/m for C band).

### Spherical Cavity

For the spherical cavity, two degenerated  $TE_{114}$  have been chosen as operating modes for their high high unloaded  $Q$  factor of about  $134000$ . The radius  $a = 118$  mm can be retrieved by the relation  $a = \frac{u_{14}c}{2\pi f}$  where  $u_{14}$  is the fourth root of the spherical Bessel function  $\hat{J}_1(x)$ ; The unloaded quality factor is  $Q_0 \approx \frac{a}{\delta}$  (where  $a$  is the radius of the cavity and  $\delta$  is the skin depth). The simulated eigenmodes (two degenerate  $TE_{114}$  modes and the  $TE_{014}$ ) obtained for the spherical resonator are shown in Fig. 4. The two  $TE_{114}$

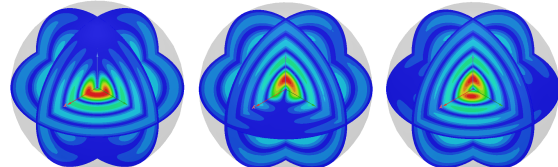


Figure 4: Electric Field patterns of the operating modes calculated using CST Eigenmode solver. From left to right the  $TE_{014}$  and the two degenerate  $TE_{114}$  modes can be observed.

modes, employed in the spherical pulse compressor have the same patterns but rotated of  $90^\circ$  as it can be seen in figure 4. In the real “final” cavity, they could be slightly distinguished due to the perturbation but a proper tuning will be implemented to obtain the two modes exactly at the operating frequency. The  $TE_{014}$  mode is higher in frequency and very weakly excited since the electric field pattern has an odd symmetry with respect to the  $\theta$  angular dependence, with the null point in the coupling iris placement area.

### Complete Pulse Compressor

After the simulation of the 3 dB coupler, the spherical cavity has been connected to simulate the complete pulse compressor. The Waveguide-to-cavity coupling is obtained thanks to a special coupling iris, placed between the circular waveguide section of the polarizer and the spherical cavity.

The iris radius has been tuned in order to get a value of  $\beta \simeq 8$ , resulting  $r_{iris} = 11$  mm. The 3D model and the electrical field distribution of the pulse compressor is shown in Fig. 5. The field distribution meets the  $TE_{114}$  mode.

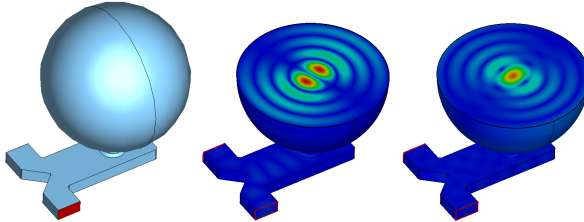


Figure 5: 3D vacuum model of the complete pulse compressor plus electric and magnetic field distribution of the  $TE_{114}$  mode along a spherical cavity slice.

The simulated S-Parameters of the pulse compressor by CST Frequency Domain Solver are shown in Fig. 6. The minimum value of  $|S_{21}|$  is about 0.7772 at the frequency  $f_0 = 5.71$  GHz, from which, as said, the coupling coefficient  $\beta$  is calculated to be about 8. The operating frequency tuning will be performed both using a matching a ridge in the sphere equator (before brazing) and with a push-pull tuning (after brazing).

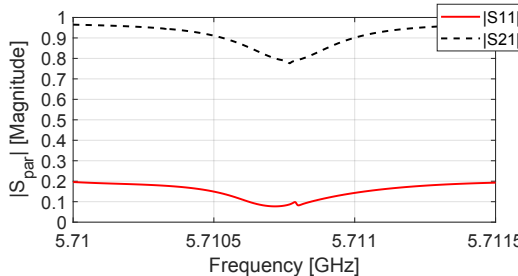


Figure 6: CST frequency domain method Simulated S-parameters  $|S_{21}|$  and  $|S_{11}|$  of the complete pulse compressor.  $TE_{114}$  mode is coupled with  $\beta \sim 8$ .

Finally, the temperature increase under pulsed operation has been evaluated considering an input power equal to 50 MW and a RF pulse length (coming from the klystron)  $\tau_p = 3 \mu s$ , as reported in Tab. 2. In this case, the maximum absolute value of the magnetic field is reached in the coupling iris area and is evaluated  $H_{max} \simeq 0.25$  MA/m, leading to a temperature increase  $\Delta T \simeq 33$  °C, that is below the imposed limit of 40 °C [12].

### Simulated Power Gain and Accelerating gradient

The considered traveling-wave constant-impedance accelerating structure is 0.9 m long, has a shunt impedance per unit length  $Z_s = 100$  MΩ/m, a filling time  $T_f = 300$  ns (group velocity of 1 % speed of light) and attenuation factor  $\alpha=0.5$  Neper. The output waveforms obtained with a RF pulse duration of 3  $\mu s$  and a phase flip of 180° in the last 300 ns [5] are shown in Fig. 7: the output power (orange) shows a peak power gain above 7 while the average power

gain is 4.7. The main specifications of the spherical cavity pulse compressor are summarized in Table 2.

Table 2: Main Specifications of the Pulse Compressor

Parameter	Design Value
Resonant frequency [GHz]	5.712
Operating mode	$TE_{114}$
Unloaded Quality Factor $Q_0$	134000
Coupling coefficient $\beta_c$	8
RF input pulse length [ $\mu s$ ]	3
RF compressed pulse length [ $\mu s$ ]	0.3
Peak power gain	7.4586
Average power gain <sup>1</sup>	4.6735

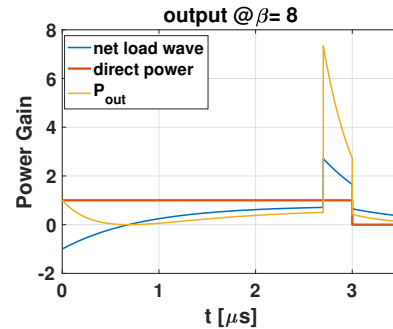


Figure 7: Input direct power (red curve), output net load wave electric field (light-blue curve) and output power  $P_{out}$  (orange curve)

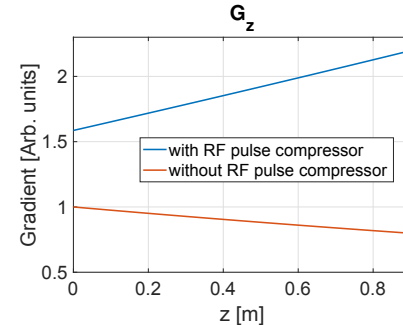


Figure 8: Accelerating gradient along the traveling wave structure without and with the RF pulse compressor.

Figure 8 shows the gradient distribution (computed according the equation (11) of [13]) without and with the RF pulse compressor which as expected enhances the gradient of the accelerating structure.

### ACKNOWLEDGEMENTS

The support of the INFN 5th National Committee is warmly acknowledged through the FRIDA call.

<sup>1</sup> on the filling time of the accelerating structure  $t_f=300$  ns

## REFERENCES

- [1] E. Schüler *et al.*, "Very high-energy electron (VHEE) beams in radiation therapy; treatment plan comparison between VHEE, VMAT, and PPBS," *Medical Physics*, vol. 44, no. 6, pp. 2544–2555, 2017.  
doi:<https://doi.org/10.1002/mp.12233>
- [2] V. Favaudon *et al.*, "Ultrahigh dose-rate FLASH irradiation increases the differential response between normal and tumor tissue in mice," in *Sci Transl Med*, vol. 6, no. 245, 245ra93, 2014.
- [3] L. Faillace *et al.*, "Perspectives in linear accelerator for FLASH VHEE: Study of a compact c-band system," *Physica Medica: European Journal of Medical Physics*, vol. 104, pp. 149–159, 2022.  
doi:[10.1016/j.ejmp.2022.10.018](https://doi.org/10.1016/j.ejmp.2022.10.018)
- [4] L. Giuliano *et al.*, "Preliminary Studies of a Compact VHEE Linear Accelerator System for FLASH Radiotherapy," in *Proc. IPAC'21*, Campinas, SP, Brazil, 2021, paper MOPAB410, pp. 1229–1232.  
doi:[10.18429/JACoW-IPAC2021-MOPAB410](https://doi.org/10.18429/JACoW-IPAC2021-MOPAB410)
- [5] Z. D. Farkas, H. A. Hoag, G. A. Loew, and P. B. Wilson, "SLED: A Method of Doubling SLAC's Energy," in *9th International Conference on High-Energy Accelerators*, 1974, pp. 576–583.
- [6] Z. D. Farkas, "Binary Peak Power Multiplier and Its Application to Linear Accelerator Design," *IEEE Trans. Microwave Theor. Tech.*, vol. 34, p. 1036, 1986.  
doi:[10.1109/TMTT.1986.1133493](https://doi.org/10.1109/TMTT.1986.1133493)
- [7] P. B. Wilson, Z. D. Farkas, and R. D. Ruth, "Sled ii: A new method of rf pulse compression," 1990.
- [8] I. V. Syratchev, "The Progress of X-Ban "Open" Cavity RF Pulse Compression Systems," 1994. <https://cds.cern.ch/record/921874>
- [9] J. Wang, S. Tantawi, and C. Xu, "Super-Compact SLED System Used in the LCLS Diagnostic System," in *27th International Linear Accelerator Conference*, 2014, THPP125.
- [10] Y. Ohkubo, H. Yonezawa, T. Shintake, H. Matsumoto, and N. Akasaka, "The C band 50-MW klystron using traveling wave output structure," in *19th International Linear Accelerator Conference*, 1998.
- [11] J. Lei *et al.*, "RF Study And Cold Test of an S-band Spherical Cavity Pulse Compressor," in *9th International Particle Accelerator Conference*, 2018.  
doi:[10.18429/JACoW-IPAC2018-WEPMF033](https://doi.org/10.18429/JACoW-IPAC2018-WEPMF033)
- [12] J. W. Wang *et al.*, "Development for a supercompact X-band pulse compression system and its application at slac," *Phys. Rev. Accel. Beams*, vol. 20, p. 110401, 11 2017.  
doi:[10.1103/PhysRevAccelBeams.20.110401](https://doi.org/10.1103/PhysRevAccelBeams.20.110401)
- [13] J.-Y. Liu *et al.*, "Analytic rf design of a linear accelerator with a sled-i type rf pulse compressor," *Nuclear Science and Techniques*, vol. 31, no. 11, p. 107, 2020.  
doi:[10.1007/s41365-020-00815-5](https://doi.org/10.1007/s41365-020-00815-5)